Degradable and biocompatible nanoparticles decorated with cyclic RGD peptide for efficient drug delivery to hepatoma cells in vitro.

Pascal Loyer, Wahib Bedhouche, Zhi Wei Huang, Sandrine Cammas-Marion

Degradable and Biocompatible Nanoparticles Decorated with Cyclic RGD Peptide for Efficient Drug Delivery to Hepatoma Cells *In Vitro*

Pascal Loyer[1], Wahib Bedhouche[1], Zhi Wei Huang[2,§], Sandrine Cammas-Marion[2,*].

[1] Inserm UMR S-991, Foie, Métabolismes et Cancer; Université de Rennes 1; Fédération de Recherche de Rennes Biosit; CHU Rennes, 35033 Rennes, France.

[2] UMR 6226 CNRS; Institut des Sciences Chimiques de Rennes; Université de Rennes 1; ENSCR, Avenue du Général Leclerc, CS 50837, 35 708 Rennes Cedex 7, France.

[§] Current address: UMR 6270 CNRS; Laboratoire Polymères Biopolymères Surfaces; Université de Rouen, 76821 Mont Saint Aignan, France.

***** Author to whom correspondence should be addressed

e-mail: sandrine.marion.1@ensc-rennes.fr; Tel: +33 2 23 23 81 09; Fax: +33 2 23 23 80 46.

Keywords: Biotinylated nanoparticles; site-specific targeting; anti-cancer drug encapsulation; degradable poly(benzyl malate) derivatives; cyclic RGD peptide; HepaRG hepatoma cells.

ABSTRACT

Amphiphilic derivatives of poly(benzyl malate) were synthesized and characterized with the aim of being used as degradable and biocompatible building blocks for the design of functional nanoparticles (NPs). An anti-cancer model drug, doxorubicin, has been successfully encapsulated into the prepared NPs and its release profile has been evaluated in water and in culture medium. NPs bearing biotin molecules were prepared either for site-specific drug delivery via the targeting of biotin receptors overexpressed on the surface of several cancer cells, or for grafting biotinylated cyclic RGD peptide onto their surface using the strong and highly specific interactions between biotin and the streptavidin protein. We have shown that this binding did not affect dramatically the physico-chemical properties of the corresponding NPs. Cyclic RGD grafted fluorescent NPs were more efficiently uptaken by the

HepaRG hepatoma cells than biotinylated fluorescent NPs. Furthermore, the targeting of HepaRG hepatoma cells with NPs bearing cyclic RGD was very efficient and much weaker for HeLa and HT29 cell lines confirming that cyclic RGD is a suitable targeting agent for liver cells. Our results also provide a new mean for rapid screening of short hepatotropic peptides in order to design NPs showing specific liver targeting properties.

1. Introduction

Nanotechnology, especially nanomedicine corresponding to the use of nanoparticles (NPs) in biomedicine, is currently an ever growing scientific and technological domain [Psimidas et al., 2012; Garanger et al., 2012]. The main reason for this unprecedented development relies on the aim to improve both early detection and treatment of numerous pathologies such as cancers. The encapsulation of a selected biologically active molecule into NPs might result in an increased drug bioavaibility within solid tumors, arising from a decrease in its non-specific recognition by the reticuloendothelial system (RES) and an improvement of its *in vivo* specific biodistribution, as well as a minimized toxicity against healthy tissues and organs [Yan et al., 2012; Elsaesser et al., 2012; Lamprecht, 2008]. Knowing that cancer, characterized by an abnormal and anarchical cell proliferation within normal tissue, is a very complex disease and a major cause of mortality [Misra et al., 2010], the development of efficient nanomedicine is thus a major challenge for public health [Reddy et al., 2011]. In this context, several anti-cancer drug loaded NPs such as Doxyl® and Abraxane® have been approved by the Food and Drug Administration (FDA) for clinical uses [Yan et al., 2012; Wang et al., 2012; Jain et al., 2010]. However besides these encouraging results, several challenges have to be overcome in order to obtain NPs allowing highly efficient site-specific drug delivery.

The materials constituting the NPs have to respect very strict specifications: they must be (i) biocompatible and non-toxic, (ii) (bio)degradable into non-toxic low molecular weight molecules or, at least, bioassimilable after releasing the encapsulated drug, (iii) undetectable by the RES meaning having stealth properties, (iv) adapted for carrying large amounts of drug that should be released in a

controlled manner at its site of action (targeting). Within this context, we have recently developed a family of degradable non-toxic polymers derived from poly(malic acid), PMLA, which are able to form well-defined NPs [Huang et al., 2012]. We have selected PMLA as macromolecular backbone because this polymer, originally synthesized for application in the biomedical field, has been successfully used as a platform in the synthesis of nanovectors [Huang et al., 2012; Cammas et al., 2000; Cammas-Marion et al., 2000; Osanai et al., 2000; Martinez Barbosa et al., 2004; Abdellaoui et al., 1998] and macromolecular conjugates [Ding et al., 2010; Ljubimova et al., 2008; Fujita et al., 2007; Fujita et al., 2006]. PMLA is known to be non-toxic and degradable into malic acid under physiological conditions [Vert et al., 1979] and its derivatives are accessible from naturally occurring PMLA [Ljubimova et al., 2008] or by anionic ring-opening polymerization (ROP) of β-substituted β-lactones [Cammas et al., 1996; Cammas et al., 1993]. PMLA derivatives used for the formulation of NPs were obtained by ROP of benzyl malolactonate (MLABe) in presence of either tetraethylammonium benzoate, α-methoxy ω-carboxy poly(ethylene glycol) -PEG_{42}-CO_2H- or α-biotin ω-carboxy poly(ethylene glycol) -Biot-PEG_{62}-CO_2H- as initiator [Huang et al., 2012]. Starting from these three PMLA derivatives, we were able to obtain well-defined non-toxic NPs in which the doxorubicin (Dox), and a fluorescent probe, the DiD oil, have been successfully encapsulated for *in vitro* assays [Huang et al., 2012]. It is worth noting that PEG has been selected as hydrophilic block because it is a well-known polymer conferring stealth properties at nanoparticles on which it is grafted [Romberg et al., 2008]. On the other hand, biotin has been chosen firstly because it is a targeting agent of certain cancer cells [Le Droumaguet et al., 2012; Patil et al., 2099; Kim et al., 2007] and secondly because it is able to interact strongly with streptavidin [Yang et al., 2009] which is an important property for our study as it will be explained afterwards in this paper.

Hepatocellular carcinoma (HCC) is the main primary malignant tumor of the liver representing 80 to 90% of liver tumors. It is the fifth most common tumor worldwide (5.4% of new cancer cases per year) and the third in term of mortality (8.2% of all cancer death) [Parkin et al., 2005]. Early detection and classification of HCC are crucial for the choice and effectiveness of therapeutic strategy. For small size

HCC, surgical treatment (resection and liver transplantation) is the most effective treatment [Hasegawa et al., 2009; Mazzeferro et al., 2008; Ishikawa et al., 1992]. Palliative treatments such as chemoembolization [Bernades-Genisson et al., 2003] and, more recently, chemotherapy using an inhibitor of tyrosine kinase, Sorafenib (Nexavar®) are proposed to patients with advanced HCC. Despites these advances, the therapeutic options for the treatment of HCC remains limited partly due to the chemoresistance of liver tumors to conventional anti-tumor agents. Therefore, the use of nanocarriers containing anti-tumor drugs has been envisaged for the treatment of HCC in order to increase the intra-hepatic drug concentration while limiting the exposure of healthy tissues and side effects [Reddy et al., 2011]. Several formulations are currently undergoing clinical trials in phase II and III such as NPs of poly(alkyl cyanoacrylate) loaded with doxorubicin (Trandrug®) for HCC treatment [Barraud et al., 2005]. In a first step, the passive accumulation of nanocarriers in the RES cells (endothelial and Kupffer cells) [Lanaerts et al., 1984] was utilized for liver targeting with a real relevance for diseases involving liver Kupffer cells such as parasitic diseases [Alving et al., 1978]. Conversely, liver targeting based on the nanocarrier's uptake by Kupffer cells has the major drawback of allowing only a low hepatic accumulation of nanocarriers since Kupffer cells represent only a few percent of liver cell volume against 90% for hepatocytes. In addition, the accumulation of nanocarriers in Kupffer cells does not target the cells responsible for HCC thus limiting the use of this approach in this case. Therefore, to overcome this drawback, active hepatocyte targeting has been studied. Most of the proposed strategies are based on the binding of NPs to the asialoglycoprotein receptors [Wu et al., 2002]. These NPs are usually liposomes incorporating glycosylated proteins or galactose/lactose linked to lipophilic anchors [Wu et al., 2002]. To date, very few nanovectors, especially polymer-based NPs, carrying peptides with high tropism for the liver have been developed [Reddy et al., 2011].

In this paper, we report, first, the monitoring of Dox release from NPs prepared from PEG_{42}-*b*-PMLABe or Biot-PEG_{62}-*b*-PMLABe in water and in culture medium at 37°C. Second, we have grafted fluorescein amine (FA) molecule at the free end of the PMLABe block of PEG_{42}-*b*-PMLABe or Biot-PEG_{62}-*b*-PMLABe block copolymers in order to obtain fluorescent NPs for *in vitro* cell uptake assays.

Starting from the corresponding fluorescent NPs, we have studied the influence of the nature of molecules localized at NPs' surfaces [PEG_{42}, Biot-PEG_{62} or Arginine-Glycine-Aspartic acid (RGD) peptide-Biot-Streptavidin-Biot-PEG_{62}] on their internalization into cells *in vitro* and demonstrated that the uptake by HepaRG hepatoma cells is considerably enhanced by the grafting of the RGD peptide onto NPs. These results also show that these biotinylated NPs can be useful tools for rapid *in vitro* screen and selection of highly hepatotropic peptides with the ultimate goal to design nanomedicine targeting hepatocytes from HCC *in vivo*.

2. Materials and methods

2.1. Materials

All chemicals were used as received. Anhydrous THF was obtained by distillation over sodium/benzophenone under N_2 atmosphere.

Three cell lines have been selected within the frame of this project: the HepaRG hepatoma cells [Gripon at al., 2002; Laurent et al., 2010;], the colorectal adenocarcinoma cell line HT29 [Fogh et al., 1975] and the cervical cancer cell line HeLa [Rahbari et al., 2009].

2.2. Apparatus

Nuclear magnetic resonance spectra (^{1}H NMR) were recorded on a Brucker ARX 400 instrument (^{1}H at 400 MHz). Data are reported as follows: chemical shift (multiplicity, number of hydrogen). The chemical shifts (δ) are reported as parts per million (ppm) referenced to the appropriate residual solvent peak. Abbreviations are as follows: *s* (singlet), *d* (doublet), *t* (triplet), *q* (quartet), *dd* (doublet of doublet), *m* (multiplet).

The size (average diameter obtained by the cumulant result method), polydispersity and zeta potential of the formulations were measured by dynamic light scattering using a Delsa™ Nano Beckman Coulter apparatus at 25°C.

UV spectra were recorded on a Secoman apparatus at 485 nm.

2.3. Synthesis of PEG_{42}-b-PMLABe and Biot-PEG_{62}-b-PMLABe

The monomer, the benzyl malolactonate (MLABe), was synthesized from DL-aspartic acid according to the previously reported synthesis [Cammas et al., 1996]. The PEG_{42}-*b*-PMLABe and Biot-PEG_{62}-*b*-PMLABe block copolymers were obtained by anionic ring opening polymerization of MLABe in presence of, respectively, α-methoxy ω-carboxy poly(ethylene glycol), PEG_{42}-CO_2H, and α-biotin ω-carboxy poly(ethylene glycol), Biot-PEG_{62}-CO_2H, as initiators following a protocol described elsewhere [Huang et al., 2012].

2.4. Grafting of fluorescein amine (FA)

2.4.1 Grafting of FA on the PEG_{42}-b-PMLABe block copolymer (Scheme 1)

The PEG_{42}-*b*-PMLABe block copolymer (500 mg) was dissolved into 1 mL of anhydrous CH_2Cl_2 under nitrogen atmosphere. To this solution were added 5 mg (1eq.) of *N,N'*-diclohexylcarbodiimide (DCC) dissolved in 1 mL of anhydrous CH_2Cl_2 followed by 7.5 mg (1eq.) of N-hydroxysuccinimide (NSH) dissolved in 1 mL of anhydrous CH_2Cl_2. The mixture was stirred under nitrogen atmosphere for 24 hours at room temperature (RT). The resulting PEG_{42}-*b*-PMLABe-NHS was precipitated in cold heptane. After the elimination of the supernatant, the precipitate was dissolved in CH_2Cl_2 and the solution was filtrated on celite. The CH_2Cl_2 was eliminated under vacuum and the activated block copolymer polymer (480 mg) was obtained with 96% yield. The activated block copolymer (480 mg) was then dissolved in 1 mL of anhydrous CH_2Cl_2. To this solution was added 12 mg of FA (1eq.) solubilised into a mixture of 1 mL of anhydrous CH_2Cl_2 and 1 mL of acetone HPLC grade under nitrogen atmosphere. After stirring at RT for 24 hours, the solution containing the PEG_{42}-*b*-PMLABe-FA block copolymer was precipitated into cold heptane. After removing the supernatant, the precipitate was dissolved into DMSO. This DMSO solution was poured into a dialysis bag (MWCO 3,500 Da) and the dialysis was conducted during 8 hours against DMSO. The solution contained into the dialysis bag was lyophilized and the PEG_{42}-*b*-PMLABe-FA block copolymer was recovered with 60% yield. The polymer was characterized by ^1H NMR in deuterated DMSO.

^{1}H NMR (d6-DMSO, δ ppm): 2.92 (s, 2nH, $CO_2\underline{CH_2}C_6H_5$), 3.32 (m, 4mH (m=42), $(\underline{CH_2CH_2}O)_{42}$), 5.10 (m, 2nH, $CH\underline{CH_2}CO_2$), 5.42 (m, 1nH, $\underline{CH}CH_2CO_2$), 6.50-7.00 (m, 9H, FA); 7.31 (m, 5nH, $CO_2CH_2\underline{C_6H_5}$).

M_{NMR} = 11,000 g/mol for the PMLABe block

2.4.2 Grafting of FA on the Biot-PEG_{62}-b-PMLABe block copolymer (Scheme 1)

The grafting of FA on the Biot-PEG_{62}-*b*-PMLABe block copolymer was realized as described above. The Biot-PEG_{62}-*b*-PMLABe-FA block copolymer was obtained with 58% yield and characterized by ^{1}H NMR in DMSO.

^{1}H NMR (d6-DMSO, δ ppm): 2.92 (s, 2nH, $CO_2\underline{CH_2}C_6H_5$), 3.37 (m, 4mH (m=62), $(\underline{CH_2CH_2}O)_{62}$), 5.07 (m, 2nH, $CH\underline{CH_2}CO_2$), 5.41 (m, 1nH, $\underline{CH}CH_2CO_2$), 6.50-7.00 (m, 9H, FA); 7.26 (m, 5nH, $CO_2CH_2\underline{C_6H_5}$). Peaks corresponding to the biotin are either under peaks correspoonding to the PEG and PMLABe blocks or too small to be detectable on the NMR spectrum.

M_{NMR} = 6,000 g/mol for the PMLABe block.

2.5. Preparation of NPs

2.5.1. Dox encapsulation and release from NPs

The protocol for Dox encapsulation and for the monitoring of its release was the same whatever the nature of the block copolymer constituted the NPs. The encapsulation of Dox into the NPs was realised as described previously [Huang et al., 2012]. Briefly, the Dox hydrochloride (Dox,HCl, Sigma) was encapsulated into the two kinds of NPs during the nanoprecipitation procedure. The selected polymer (5 mg) was dissolved in acetone (1 mL). Two hundred µL of a Dox solution [1.5 mg of Dox,HCl solubilised in 0.6 mL of a mixture of chloroform (6 mL) and NEt_3 (23 µL)] were added to the polymer solution. This mixture was then nanoprecipitated into 2 mL of water under vigorous stirring. After organic solvent evaporation, the unloaded Dox was removed by ultracentrifugation at 15,000 g at 15°C for 7 min using filter with an exclusion limit 10,000 Da. The filters were returned and centrifuged for 1

min at 1,000 g at 15°C. The volume of the recovered solutions was completed to 2 mL with distilled water in order to obtain a final concentration in NPs of 2.5 g/L. The concentration of loaded Dox was evaluated by UV at 485 nm, as described elsewhere [Huang et al., 2012; Cammas et al., 1995]. Briefly, 200 µL of Dox-loaded NPs were dissolved into 800 µL of DMF and the resulting solutions were analyzed by UV at 485 nm. The absorbance of Dox encapsulated into NPs was converted into a concentration using a calibration curve and the encapsulation efficiency (e.e.) was calculated using the following equation:

$$\text{e.e.} = \frac{[\text{Total drug}] - [\text{Free drug}]}{[\text{Total drug}]} \times 100$$

The characteristics of the Dox-loaded NPs (diameter, polydispersity index and zeta potential) were measured using the Delsa™ Nano Beckman Coulter apparatus (Table 1).

The Dox release from both kinds of NPs were monitoring by dialysis in water and in culture medium at 37°C. The protocol used in both cases was identical. Two mL of the Dox-loaded NPs solution were placed into a dialysis bag (MWCO = 3,500 Da); this bag was then incubated into 40 mL of water or culture medium maintained at 37°C. After different incubation time, from 30 min up to 72 hours, 2 mL of the outside solution are taken and replaced by 2 mL of fresh water or culture medium. For each sample, 200 µL of the collected outside solution were analyzed by UV at 485 nm and the quantity of Dox was determined thanks to calibration curves previously realized in water and in culture medium by UV measurements at 485 nm.

2.5.2. Preparation of fluorescent NPs

The fluorescent NPs were prepared by the nanoprecipitation technique as previously described [Thioune et al., 1997; Huang et al., 2012]. Briefly, the mixture of PEG_{42}-*b*-PMLABe-FA (2.5 mg) and PEG_{42}-*b*-PMLABe (2.5 mg) or Biot-PEG_{62}-*b*-PMLABe-FA (2.5 mg) and Biot-PEG_{62}-*b*-PMLABe (2.5 mg) were dissolved in 1 mL of acetone. This solution is added to 2 mL of water under vigorous stirring. The organic solvent (acetone) was then evaporated under vacuum and the final volume was

completed to 2 mL with fresh water. The final concentration in block copolymers under NPs' form was 2.5 g/L. The solutions containing the fluorescent NPs were characterized by dynamic light scattering using a Delsa™ Nano Beckman Coulter apparatus at 25°C (Table 2).

2.5.3. Grafting of the cyclic RGD peptide

The selected biotinylated peptide, the cyclic Biot-RGD peptide (Eurogentec, Belgium), was grafted onto the biotinylated NP's surfaces via the streptavidin (Strept, AnaSpect, Eurogentec, Belgium) protein. An aqueous solution of Biot-RGD peptide was prepared at a final concentration of 2.9 mM. In parallel, an aqueous solution of streptavidin was also prepared with a final concentration of 178 µM. The Biot-RGD peptide (2.7 µL) and the streptavidin (22 µL) solutions were mixed in a final volume of 50 µL (H_2O qsp) and incubated for 1 hour at 4°C. Then, the Biot-PEG_{62}-*b*-PMLABe-FA or Biot-PEG_{62}-*b*-PMLABe based NP's solution (35 µL), previously prepared, was added to a final volume of 100 µL (H_2O qsp). This mixture was incubated for 1 hour and diluted to a final volume of 1 mL in culture medium for final concentrations of the Biot-RGD peptide at 8µM, the streptavidin at 4µM and polymers at 4µM. In order to demonstrate that both the Biot-RGD peptide grafting and the dilution have no influence on NP's characteristics, we analyzed the NPs formed in the conditions described above by DLS (Table 3).

2.6. Cell uptake assays

The cell lines, HT29 [Fogh et al., 1975] and HeLa [Rahbari et al., 2009], were cultured as described in the literature. The HepaRG cell line was cultured in the medium William's E (Lonza) supplemented with 2mM of glutamine (Gibco), 5 mg/L of insulin (Sigma), 10^{-5} M hydrocortisone hemisuccinate and 10% of fetal calf serum (Lonza) [Gripon at al., 2002; Laurent et al., 2010]. During the sub-culturing, 2.10^6 cells were seeded in a 75 cm^3 flask. The medium was renewed every 48 hours. The sub-culturing was realized by trypsinization every 2 weeks in order to maintain the progenitor phenotype. For an

optimal differentiation, the cells were maintained at confluence after the two weeks and the medium was supplemented with 2% of dimethylsulfoxide (DMSO) [Laurent et al., 2013].

For the cell uptake assays, the 24 wells culture plates were seeded with the selected cell line (HepaRG, HT29 or HeLa) with 10^5 cells per well. Then the NPs' preparations (4µM of block copolymer under NPs' form ± 4 µM streptavidin and 8 µM Biot-RGD) or a negative control (buffer without NPs or non fluorescent NPs) were added to the wells. For the competitive experiments, the cells were pre-treated with an excess of free RGD peptide (32 µM).

The cells were incubated from 1 to 24 hours. After incubation, the culture medium was removed; the cell monolayers were washed with PBS before the observation by fluorescence microscopy (Zeiss inverted microscope, analysis software AxioVision). Then the cells were detached with trypsin and analyzed by flow cytometry (FACSCalibur Becton Dikinson) to quantify the fluorescence (Channel FL1H) emitted by the fluorescent NPs captured by the cells. Cytometry data were analyzed using CellQuest software (Becton Dikinson).

3. Results and Discussion

In order to further characterize the PMLABe based NPs as drug nanocarriers for applications in nanomedicine, we (i) studied the release of Dox in water and culture medium at 37°C, (ii) grafted a fluorescent probe at the free end of the hydrophobic PMLABe block for studying *in vitro* cellular uptake and (iii) evaluated the possibility to build a molecular scaffold by grafting the cyclic RGD-biotinylated peptide onto biotinylated NPs via the streptavidin as a bridging factor and determine the impact of the RGD peptide addition on cell uptake.

Figure 1

3.1. *Dox encapsulation and release from NPs*

Both Dox-loaded PEG_{42}-*b*-PMLABe and Biot-PEG_{62}-*b*-PMLABe based NPs have been prepared by the nanoprecipitation technique and have been characterized by DLS. Table 1 collects the results obtained for PEG_{42}-*b*-PMLABe and Biot-PEG_{62}-*b*-PMLABe based NPs. Initial Dox content in both NPs determined by UV at 485 nm as described previously [Huang et al., 2012] showed an encapsulation efficiency ranging from 32 to 36%.

Table 1

The release of Dox from both PEG_{42}-*b*-PMLABe and Biot-PEG_{62}-*b*-PMLABe NPs in water and in culture medium was realized at 37°C by dialysis. Aliquots of the external solution (outside the dialysis bag) were collected after various incubation times and analyzed by UV at 485 nm and confirmed that the Dox was encapsulated with an efficiency of nearly 35% (Table 1). As shown in figure 2, Dox release profiles from both types of NPs in water (Figure 2, A) and in the culture medium (Figure 2, B) are quite similar.

Figure 2

The release, expressed as a percentage of the total amount of encapsulated Dox, is nearly 5% after one hour of incubation. This release accelerates after the second hour to reach 40% after 6 hours of incubation in both water and culture medium. Then the release reaches a plateau around 55 to 60% from 24 to 72 hours of incubation. The fast release of Dox within the first hours is probably due to the Dox absorbed in the hydrophilic PEG corona. Indeed, Dox is known to be an amphiphilic molecule which is therefore spread from the hydrophilic corona to the surface of the hydrophobic core of the nanoparticles. However to conclude regarding the exact location of the Dox in the PEG-*b*-PMLABe forming NPs, it will be necessary to realize further experiments such as X-ray measurements.

Nevertheless, these results are quite encouraging because we are able to encapsulate substantial amount of this drug and the release profile is in agreement with the Dox amphiphilic nature.

3.2. Grafting of fluorescein amine and cellular uptake assays

Besides the use of biotin as a well-known targeting agent of cancer cells [Yang et al., 2009], we aimed at developing a versatile procedure to screen for more specific targeting agents, especially short peptides, towards transformed hepatocytes from hepatocellular carcinoma (HCC).

Our goal is to select peptides exhibiting a remarkably high tropism for the hepatocytes as targeting agents and to graft them at the surface of PMLA derivatives-based NPs in order to achieve an optimized uptake of NPs by the hepatocytes. In a first step, we wish to screen, rapidly and in a simple manner without engaging more organic chemistry, a large number of peptides which potentially show a strong hepatotropism to select the most efficient ones. For that purpose, we used the non-covalent binding of selected peptides via the strong biotin-streptavidin affinity as shown by Figure 3 [Yang et al., 2009].

Figure 3

In a first step to determine whether such a molecular scaffold could allow the production of NPs and could be used for cell uptake *in vitro*, we have selected biotinylated cyclic RDG (Arg-Gly-Asp- DTyr-Lys-Biotin) peptide, known for interacting with integrin proteins well expressed in the liver and even more in tumors rich in extracellular matrix [Jiang et al., 2011]. This biotinylated RGD peptide has been introduced after the formation of biotinylated NPs through streptavidin interactions [Yang et al., 2009]. Moreover, in order to follow the *in vitro* cellular uptake of the NPs, we have synthesized fluorescein amine grafted PEG_{42}-*b*-PMLABe and Biot-PEG_{62}-*b*-PMLABe block copolymers. As shown by scheme 1, the fluorescein amine (FA) was successfully grafted at the free carboxylic acid end of the PMLABe

block activated with N-hydroxysuccinimide (NHS) without modifying the structure of block copolymers.

Scheme 1

After purification by dialysis allowing the elimination of unreacted FA and low molecular weight side products, both block copolymers were characterized by ^{1}H NMR in deuterated DMSO. The ^{1}H NMR spectra allowed us to conclude that the structures of FA-modified block copolymers were in agreement with the expected ones and that the molecular weights of PMLABe blocks calculated from the ^{1}H NMR spectra were identical to the ones of initial materials.

Starting from a mixture of the fluorescent block copolymers and the non-fluorescent ones (50/50 wt%), we have then prepared the corresponding fluorescent NPs using the nanoprecipitation method [Huang et al., 2012; Thioune et al., 1997]. The obtained NPs were characterized by dynamic light scattering. As shown by results gathered in table 2, the presence of FA molecules at the end of the PMLABe block has no significant influence on the NP's diameters and polydispersity indices.

Table 2

Biotinylated cyclic RGD peptide was then associated with NPs formed by a mixture of Biot-PEG_{62}-b-PMLABe-FA and Biot-PEG_{62}-b-PMLABe (50/50 wt%) using streptavidin, a tetrameric protein of 56 KDa purified from the bacterium *Streptomyces avidinii*, as an intermediate link between the biotin localized on the surface of preformed polymeric NPs and the biotinylated peptide (Figure 3). The dissociation constant (Kd) of the biotin/streptavidin complex is on the order of 10^{-15} mol/L, ranking among the strongest known non-covalent interactions [Yang et al., 2009]. The non-covalent binding of RGD modified fluorescent NPs was realized by first mixing the biotinylated RGD peptide with the streptavidin followed by the addition of this complex to biotinylated fluorescent NPs. The relative

amounts of block copolymers constituting the NPs, RGD peptide and streptavidin can have a significant influence on the cell capture. Therefore, different amounts of block copolymer constituting the NPs, RGD peptide and streptavidin were tested and the cell uptake was measured by fluorescent microscopy and flow cytometry (Data not shown); the best results were obtained with the following conditions: 4 µM of block copolymers under NP's form, 4 µM of streptavidin and 8 µM of biotinylated RGD peptide.

The diameter and polydispersity index of unmodified and modified NPs were measured by DLS in order to demonstrate that the addition of RGD-Biot-streptavidin construct and the dilution had no influence on the properties of the corresponding NPs. As shown by results gathered in table 3, the dilution of Biot-PEG_{62}-b-PMLABe NPs either in PBS or in culture medium with or without serum does not have a significant influence on both the diameter and the polydispersity index values, meaning that the polymers constituting the NPs are still associated under NP's form.

Table 3

The addition of the Strep-Biot-RGD construct on the biotinylated NPs has led to a moderated increase in the NPs' diameter and polydispersity indices. For NPs resuspended either in PBS or culture medium with serum the emergence of a second peak centered at 600 nm and 970 nm, respectively, was observed. Such results indicate that addition of Strep-Biot-RGD construct does not lead to the destabilization of the NPs but rather a moderate formation of aggregates. However, such limited modifications were considered acceptable for cell uptake *in vitro* assays. It is important to note that RGD modified NPs were stable for at least 48 hours when stored at room temperature as shown by values of diameters and polydispersity indices unchanged (measures realized by DLS, data not shown).

We then realized *in vitro* assays of cell captation using the human hepatoma HepaRG cell line [Laurent et al., 2010; Gripon et al., 2002]. HepaRG cells were incubated for 24 hours in the presence of biotinylated NPs modified or not with the RGD-Biot-Streptavidin construct with final concentrations

in culture media of 4 µM of block copolymers, 4 µM of streptavidin and 8 µM of RGD peptide. The cell uptake was studied by Facs and fluorescent microscopy (Figure 4).

Figure 4

The Facs analysis showed that the peak of fluorescence in cells incubated with the Biot-PEG_{62}-*b*-PMLABe-FA NPs had significantly shifted on the right compared to fluorescence in control cells incubated with non fluorescent NPs demonstrating that most of the cells contained fluorescent NPs. However, the mean of fluorescence remained low (~30 arbitrary units) for Biot-PEG_{62}-*b*-PMLABe NPs and Biot-PEG_{62}-*b*-PMLABe-FA NPs, respectively, compared to the mean for cells incubated with non-fluorescent NPs. The fluorescent microscopy confirmed that HepaRG cell uptake of Biot-PEG_{62}-*b*-PMLABe-FA NPs was very limited compared to negative control cells exposed to the non-fluorescent NPs demonstrating that the biotin did not trigger a strong captation. Addition of the RGD peptide led to strong increase in the fluorescence level within HepaRG cells reaching a mean of ~1500 U.A and with over 90% of positive cells (Figure 4). These data demonstrate that the addition of the RGD peptide onto NPs has considerably enhanced the cell uptake of the NPs.

We then followed the time course of uptake by HepaRG cells of NPs formed by Biot-PEG_{62}-*b*-PMLABe-FA or Biot-RGD-Strept-Biot-PEG_{62}-*b*-PMLABe-FA by flow cytometry analysis at 2, 6, 14 and 24 hours of incubation. As shown by figure 5, the results of mean of fluorescence intensity indicated a very rapid uptake within the first 6 hours which continued slower until 24 hours for RGD-Biot-Strept-Biot-PEG_{62}-*b*-PMLABe-FA based NPs (Figure 5, red curve), while no change in the fluorescence intensity has been observed for the uptake of Biot-PEG_{62}-*b*-PMLABe-FA based NPs (Figure 5, blue curve).

Figure 5

Furthermore, we have evaluated the specificity of the uptake of RGD modified fluorescent NPs by HepaRG cells by comparing the efficiency of the uptake in absence or presence of an excess of free RGD peptide at a concentration of 34 µM (Figure 6). The results of fluorescence intensity measured by flow cytometry indicated that the pre-incubation of HepaRG cells with free RGD peptide before the addition of RGD modified fluorescent NPs strongly inhibited the cell uptake. Therefore, we can conclude that the presence of the RGD peptide at the NP's surfaces is responsible for the increase in HepaRG cell uptake of NPs.

Figure 6

In final experiment, we compared the efficiency of the uptake of RGD modified fluorescent NPs by three different cell lines: the hepatoma HepaRG, the colon HT29 and the cervical HeLa cancer cells (Figure 7).

Figure 7

The three cell lines showed low levels of fluorescence following incubation with Biot-PEG_{62}-*b*-PMLABe-FA NPs for 24 hours demonstrating that these biotinylated NPs are poorly uptaken by cells from different tissue origin. Importantly, the three cell types exhibited very different uptake of the RGD-Biot-Strept-Biot-PEG_{62}- *b*-PMLABe-FA formed NPs. The number of positive HT29 cells is very low (< 5%) while about 90% of HeLa cells captured the RGD modified fluorescent NPs (Figure 7). However, the degree of uptake (fluorescence intensity) in HeLa cells is much lower than the one observed for HepaRG cells (Figure 7). This result suggested that the number of membrane receptors binding RGD peptide (integrin family members) on HeLa cells is sufficient to trigger the uptake of NPs by most of the cells. However, the density of these receptors onto HeLa cells might be lower than

onto HepaRG cells leading to a higher degree of NPs captation by the hepatoma cells than the HeLa cells.

4. Conclusions

In this study, we have demonstrated a rapid release of the Dox from PEG_{42}-*b*-PMLABe and Biot-PEG_{62}-*b*-PMLABe NPs over the first 6 hours. However, the NPs, which are stable in water and culture medium for several days, entrapped a fraction of the drug that is slowly released over several days. Then, we characterized the cell uptake of PEG_{42}-*b*-PMLABe and Biot-PEG_{62}-*b*-PMLABe NPs using fluorescein amine modified polymers. We demonstrated that biotinylated NPs modified with the cyclic RGD peptide significantly increase the uptake by HepaRG cells in comparison to NPs formed by Biot-PEG_{62}-*b*-PMLABe-FA without peptide. We have also proved that this capture was dependent on the presence of the RGD peptide because the addition of an excess of free RGD peptide strongly inhibited the uptake. In addition, our results indicate that the RGD peptide presents a real tropism for liver cells since its uptake by HeLa and HT29 cells was much lower than the uptake by HepaRG cells. These results should be complemented by a larger study including other liver and non-hepatic cell lines as well as primary cells such as endothelial cells and normal hepatocytes. Our study also provides a proof of concept for the use of the versatile molecular scaffold presented in Figure 3 in order to screen for other short peptides targeting hepatocytes and HCC. Since we have shown that it was possible to use the streptavidin to graft a biotinylated peptide onto the biotin present at the surface of Biot-PEG_{62}-*b*-PMLABe based NPs, we are evaluating a number of peptides without having to engage additional chemistry. The most efficient peptides will be then grafted at the end of the hydrophilic PEG block to avoid the use of immunogenic streptavidin for further *in vivo* biodistribution assays.

Acknowledgments

We would like to thank Denise Glaise for culturing the HepaRG cells. This work was supported by Inserm, CNRS, the University of Rennes 1 (Défis émergents-2012) and les comités départementaux de

la Ligue contre le Cancer du GrandOuest: comités 29, 35 et 53. Z.H. H. thanks the Région Bretagne and the European University of Bretagne (UEB) for a Ph.D. grant and a 4 months mobility fellowship, respectively.

References

Abdellaoui, K., Boustta, M., Vert, M., Morjani, H., Manfait, M. 1998. Metabolite-derived artificial polymers designed for drug targeting, cell penetration and bioresorption., Eur. J. Pharm. Sci. 6, 61-73.

Alving, C.R., Steck, E.A., Chapman, W.L. Jr., Waits, V.B., Hendricks, L.D., Swartz, G.M. Jr., Hanson, W.L. 1978. Therapy of leishmaniasis: Superior efficacies of liposome-encapsulated drugs., Proc. Natl. Acad. Sci. U S A 75(6), 2959-2963.

Barraud, L., Merle, P., Soma, E., Lefrançois, L., Guerret, S., Chevallier, M., Dubernet, C., Couvreur, P., Trépo, C., Vitvitski, L. 2005. Increase of doxorubicin sensitivity by doxorubicin-loaded into nanoparticles for hepatocellular carcinoma cells in vitro and in vivo., J. Hepatol. 42(5), 736-743.

Bernades-Genisson, V., Bernadou, J., Berque-Bestel, I., Brion, J.D., Couquelet, J., Cussac, M., Debert, M., Duval, O., Giorgi-Renault, S., Huet, J., Lacroix, R., Laronze, J.Y., Le Baut, G., Loiseau, P., Nuhrich, A., Plat, M., Poisson, J., Robert-Piessard, S., Tournaire-Arllano, C., Uriac, P. 2003. In « Traité de chimie thérapeutique », vol. 6, « Médicaments anti-tumoraux et perspectives dans les traitements des cancers ». Edition TEC et DOC. 3-23.

Cammas, S., Renard, I., Boutault, K., Guérin, Ph. 1993. A novel synthesis of optically active 4-benzyloxy- and 4-alkyloxycarbonyl-2 oxetanones., Tetrahedron Asymmetry 4(8), 1925-1930.

Cammas, S., Nagasaki, Y., Kataoka, K. 1995. Heterobifunctional Poly(ethylene oxide) : Synthesis of α-methoxy-ω-amino and α-hydroxy-ω-amino PEOs with the same molecular weights., Bioconjugate Chem. 6, 226-230.

Cammas, S., Renard, I., Langlois, V., Guérin, Ph. 1996. Poly(β-malic acid): obtaining of high molecular weights by improvement of the synthesis route., Polymer 37(18), 4215-4220.

Cammas, S., Béar, M.M., Harada, A., Guérin, Ph., Kataoka, K. 2000. New macromolecular micelles based on degradable amphiphilic block copolymers., Macromol. Chem. Phys. 201(3), 355-364.

Cammas-Marion, S., Guérin, Ph. 2000. 4-Alkyloxycarbonyl-2-oxetanones and 3-alkyloxycarbonyl-2-oxetanones as versatile chiral precursors in the design of functionalized polyesters with controlled architecture., Designed Monomers and Polymers (DMP) 3(1), 77-93.

Ding, H., Inoue, S., Ljubimov, L.V., Patil, R., Portilla-Arias, J., Hu, J., Konda, B., Wawrowsky, K.A., Fujita, M., Karabalin, N., Sasaki, T., Black, K.B., Holler, E., Ljubimova, J.Y. 2010. Inhibition of brain tumor growth by intravenous poly(β-L-malic acid) nanobioconjugate with pH-dependent drug release., Proc. Natl. Acad. Sci. USA 107, 18143-18148.

Elsaesser, A., Howard, C.V. 2012. Toxicology of nanoparticles. Advanced Drug Delivery Reviews 64, 129-137.

Fujita, M., Khazenzon, N.M., Ljubimov, A.V., Lee, B.S., Virtanen, I., Holler, E., Black, K.L., Ljubimova, J.Y. 2006. Inhibition of laminin-8 in vivo using a novel poly(malic acid)-based carrier reduces glioma angiogenesis., Angiogenesis 9, 183-191.

Fujita, M., Lee, B.S., Khazenzon, N.M., Penichet, M.L., Wawrowsky, K.A., Patil, R., Ding, H., Holler, E., Black, K.L., Ljubimova, J.Y. 2007. Brain tumor tandem targeting using a combination of monoclonal antobodies attached to biopoly(β-L-malic acid)., J. Controlled Release 122 (3), 356-363.

Fogh, J., Trempe, G., 1975. In "Human Tumor Cells in Vitro", Ed. J. Fogh, Plenum, New York 115-140.

Garanger, E., Lecommandoux, S., 2012. Towards Bioactive Nanovehicles Based on Protein Polymers., Angew Chem. Int. Ed. 51, 3060-3062.

Gripon, P., Rumin, S., Urban, S., Le Seyec, J., Glaise, D., Cannie, I., Guyomard, C., Lucas, J., Trepo, C., Guguen-Guillouzo, C. 2002. Infection of a human hepatoma cell line by hepatitis B virus., Proc. Natl. Acad. Sci. USA 99(24), 15655-15660.

Hasegawa, K., Kokudo, N. 2009. Surgical treatment of hepatocellular carcinoma., Surg. Today 39(10), 833-843.

Huang, Z.W., Laurent, V., Chetouani, G., Ljubimova, J.Y., Holler, E., Benvegnu, T., Loyer, P., Cammas-Marion, S. 2012. New functional degradable and bio-compatible nanoparticles based on poly(malic acid) derivatives for site-specific anti-cancer drug delivery., Int. J. Pharm. 423, 84-92.

Ishikawa, T. 1992. The ATP-dependent glutathione S-conjugate export pump., Trends Biochem. Sci. 17(11), 463-468.

Jain, R.K., Stylianopoulos, T. 2010. Delivering nanomedicine to solid tumors., Nat. Rev. Clin. Oncol. 7(11), 653-664.

516 Jiang, X., Sha, X., Xin, H., Chen, L., Gao, X., Wang, X., Law, K., Gu, J., Chen, Y., Jiang, Y., Ren, X.,
517 Ren, Q., Fang, X. 2011. Self-aggregated pegylated poly(trimethylene carbonate) nanoparticles
518 decorated with c(RGDyK) peptide for targeted paclitaxel delivery to integrin-rich tumors.,
519 Biomaterials 32, 9457-9469.
520
521 Kim, S.Y., Cho, S.H., Lee, Y.M., Chu, L.Y. 2007. Biotin-conjugated block copolymeric nanoparticles
522 as tumor-targeted drug delivery systems. Macromol. Res. 15, 646-655.
523
524 Lamprecht, A. 2008. In : Nanotherapeutics – Drug Delivery Concept in Nanoscience, Publisher: Pan
525 Standford Publishing Pte. Ltd., World Scientific Publishing Co. Pte. Ltd., Singapore.
526
527 Lanaerts, V., Nagelkerke, J.F., Van Berkel, T.J., Couvreur, P., Grislain, L., Roland, M., Speiser, P.
528 1984. In vivo uptake of polyisobutyl cyanoacrylate nanoparticles by rat liver Kupffer, endothelial, and
529 parenchymal cells., J. Pharm. Sci. 73(7), 980-982.
530
531 Laurent, V., Fraix, A., Montier, T., Cammas-Marion, S., Ribault, C., Benvengu, T., Jaffres, P-A.
532 Loyer, P. 2010. Highly efficient gene transfer into hepatocyte-like cells: new means for drug
533 metabolism and toxicity studies., Biotechnol. J. 5, 314-320.
534
535 Laurent, V., Glaise, D., Nübel, T., Gilot, D., Corlu, A., Loyer, P. 2013. Highly Efficient SiRNA and
536 Gene Transfer into Hepatocyte-Like HepaRG Cells and Primary Human Hepatocytes. Methods Mol
537 Biol. 987, 295-314.
538
539 Le Droumaguet, B., Nicolas, J., Brambilla, D., Mura, S., Maksimenko, A., De Kimpe, L., Salvati, E.,
540 Zona, C., Airoldi, C., Canovi, M., Gobbi, M., Noiray, M., La Ferla, B., Nicotra, F., Scheper, W.,
541 Flores, O., Masserini, M., Andrieux, K., Couvreur, P. 2012. Versatile and efficient targeting using a

single nanoparticulate platform: application to cancer and Alzheimer's disease. ACS Nano 6, 5866-5879.

Ljubimova, J.Y., Fujita, M., Khazenzon, N.M., Lee, B.S., Wachsmann-Hogiu, S., Farkas, D.L., Black, K.L., Holler, E. 2008. Nanoconjugate based on polymalic acid for tumor targeting., Chem. Biol. Interact. 171, 195-203.

Martinez Barbosa, M.E., Cammas, S., Appel, M., Ponchel, G. 2004. Investigation of the degradation mechanisms of poly(malic acid) esters in vitro and their related cytotoxicities on J774 macrophages., Biomacromolecules 5, 137-143.

Mazzaferro, V., Chun, Y.S., Poon, R.T., Schwartz, M.E., Yao, F.Y., Marsh, J.W., Bhoori, S., Lee, S.G. 2008. Liver Transplantation for Hepatocellular Carcinoma., Ann. Surg. Oncol. 15(4), 1001-1007.

Misra, R., Acharya, S., Sahoo, S.K. 2010. Cancer nanotechnology: application of nanotechnology in cancer therapy., Drug Discovery Today 15(19/20), 842-850.

Osanai, S., Nakamura, K. 2000. Effect of complexation between liposome and poly(malic acid) on aggregation and leakage behaviour., Biomaterials 21, 867-876.

Parkin, D.M., Bray, F., Ferlay, J., Pisani, P. 2005. Global Cancer Statistics, 2002. CA. Cancer J. Clin. 55(2), 74-108.

Patil, Y.B., Toti, U.S., Khdair, A., Ma, L., Panyam, J. 2009. Single-step surface functionalization of polymeric nanoparticles for targeted drug delivery., Biomaterials 30, 859-866.

568 Psimadas, D., Georgoulias, P., Valotassiou, V., Loudos, G. 2012. Molecular Nanomedicine Towards
569 Cancer: 111In-labeled Nanoparticles., J. Pharm. Sci. 101(7), 2271-2280.
570
571 Rahbari, R., Sheahan, T., Modes, V., Collier, P., Macfarlane, C., Badge, R.M. 2009. A novel L1
572 retrotransposon marker for HeLa cell line identification., BioTechniques 46(4), 277–284.
573
574 Reddy, L.H., Couvreur, P. 2011. Nanotechnology for therapy and imaging of liver diseases., J.
575 Hepatology 55(6), 1461-1466.
576
577 Romberg, B., Hennink, W.E., Strom, G. 2008. Sheddable coatings for long-circulating nanoparticles.,
578 Pharmaceutical Research 25(1), 55-71.
579
580 Thioune, O., Fessi, H., Devissaguet, J.P., Puisieux, F. 1997. Preparation of pseudolatex by
581 nanoprecipitation: influence of the solvent nature on intrinsic viscosity and interaction constant., Int. J.
582 Pharm. 146, 233-238.
583
584 Vert, M., Lenz, R.W. 1979. Preparation and properties of polyβ-malic acid: a functional polyester of
585 potential biomedical importance., Polym. Prepr. (Am. Chem. Soc., Div. Polym. Chem.) 20(1), 608-
586 611.
587
588 Wang, A.Z., Langer, R., Farokhzad, O.C. 2012. Nanoparticle Delivery of Cancer Drugs., Annu. Rev.
589 Med. 63, 185-198.
590
591 Wu, J., Nantz, M.H., Zern, M.A. 2002. Targeting Hepatocytes for Drug and Gene Delivery: Emerging
592 Novel Approaches and Applications., Front. Biosci. 7, 717-725.
593

Yan, Y., Such, G.K., Johnston, A.P.R., Best, J.P., Caruso, F. 2012. Engineering Particles for Therapeutic Delivery: Prospects and Challenges., ACS Nano. 6(5), 3663-3669.

Yang, W., Cheng, Y., Xu, T., Wang, X., Wen, L.P. 2009. Targeting cancer cells with biotin-dendrimer conjugates., Eur. J. Med. Chem. 44, 862-868.

600 Table 1. Characteristics of Dox-loaded NPs.

NPs	Diameter (nm)[a]	Polydispersity index (Ip)[a]	Zeta potential (mV)[a]	Encapsulation efficiency (%)[b]
PEG_{42}-*b*-PMLABe	66 ± 7	0.22	- 8 ± 2	36 ± 3
Biot-PEG_{62}-*b*-PMLABe	74 ± 4	0.22	- 6 ± 1	32 ± 2

601 *a. Measured by DLS (Delsa™ Nano Beckman Coulter); b. Measured by UV at 485 nm.*

602

603 Table 2. Characteristics of fluorescent NPs measured by DLS (Delsa™ Nano Beckman Coulter).

NPs	Diameter (nm)	Polydispersity index
PEG_{42}-*b*-PMLABe-FA + PEG_{42}-b-PMLABe (50wt%)	64 ± 14	0.16
Biot-PEG_{62}-*b*-PMLABe-FA + Biot-PEG_{62}-b-PMLABe (50wt%)	70 ± 13	0.22

604

605

606

607

608

609

610

611

612

613

614

615

616

617

Table 3. Characteristics of NPs modified or not by the strep-Biot-RGD construct measured by DLS (Delsa™ Nano Beckman Coulter).

Conditions	NPs Biot-PEG_{62}-b-PMLABe		NPs Biot-PEG_{62}-b-PMLABe + strep-Biot-RGD	
	Diameter (nm)	Ip	Diameter (nm)	Ip
Initial (2.5 g/L)	53 ± 12	0.17	--	--
Solution in PBS (0.107 g/L)	79 ± 15	0.37	208 ± 30 [(a)]	0.35[(a)]
Solution in culture medium without serum (0.107 g/L)	78 ± 15	0.29	191 ± 21	0.28
Solution in culture medium with serum (0.107 g/L)	106 ± 30	0.15	185 ± 30 [(b)]	0.23[(b)]

(a). Presence of a second peak centered at 600 ± 100 nm; (b). Presence of a second peak centered at 970 ± 220 nm

Figure captions:

Figure 1. Uses of PMLA derivatives as building blocks for the design of versatile NPs.

Figure 2. Release profile of Dox in water (A) and in culture medium (B) at 37°C.

Figure 3. Schematic representation of the molecular scaffold following grafting of biotinylated peptide on the biotinylated NPs via streptavidin as a bridging factor.

Figure 4. Flow cytometry (right) and *in situ* fluorescence microscopy (left) analysis of HepaRG cells incubated with Biot-PEG_{62}-*b*-PMLABe NPs, Biot-PEG_{62}-*b*-PMLABe-FA NPs and RGD-Biot-Strept-Biot-PEG_{62}-*b*-PMLABe-FA NPs. For Facs analysis, size (FSC-H) and granularity (SSC-H) were visualized to select the R1 gate corresponding to living cells. Detection on fluorescent cells in the R1 gate was performed using the FL1-H channel: negative cells incubated with Biot-PEG_{62}-*b*-PMLABe NPs were set in the M1 window and positive cells were detected in the M2 window. For cells incubated with Biot-PEG_{62}-*b*-PMLABe-FA and RGD-Biot-Strept-Biot-PEG_{62}-*b*-PMLABe-FA NPs (≥) 50 and (≥) 90% of cells were fluorescent, respectively; white bar : 50 µm.

Figure 5. Time course of the uptake of NPs by HepaRG cells. Red curve: RGD-Biot-Strept-Biot-PEG_{62}-*b*-PMLABe-FA NPs; Blue curve: Biot-PEG_{62}-*b*-PMLABe-FA NPs; white bar : 50 µm.

Figure 6. Captation of fluorescent nanoparticles (24 hour incubation) by HepaRG cells in absence or in presence of free RGD peptide; Flow cytometry (Left) and fluorescence microscopy (Rigth) analyses with Biot-PEG_{62}-*b*-PMLABe-FA NPs, RGD-Biot-Strept-Biot-PEG_{62}-*b*-PMLABe-FA NPs and RGD-Biot-Strept-Biot-PEG_{62}-*b*-PMLABe-FA NPs + 34 µM of free RGD peptide. Bottom chart: Mean of fluorescence under the various tested conditions.

Figure 7. Flow cytometry measurements of fluorescence in HepaRG, HT29 and HeLa cells incubated with Biot-PEG_{62}-*b*-PMLABe-FA or RGD-Biot-Strept-Biot-PEG_{62}-*b*-PMLABe-FA formed NPs for 24 hours. Left chart: Number of positive cells; right chart: Mean of fluorescence.

652 Figure 1.

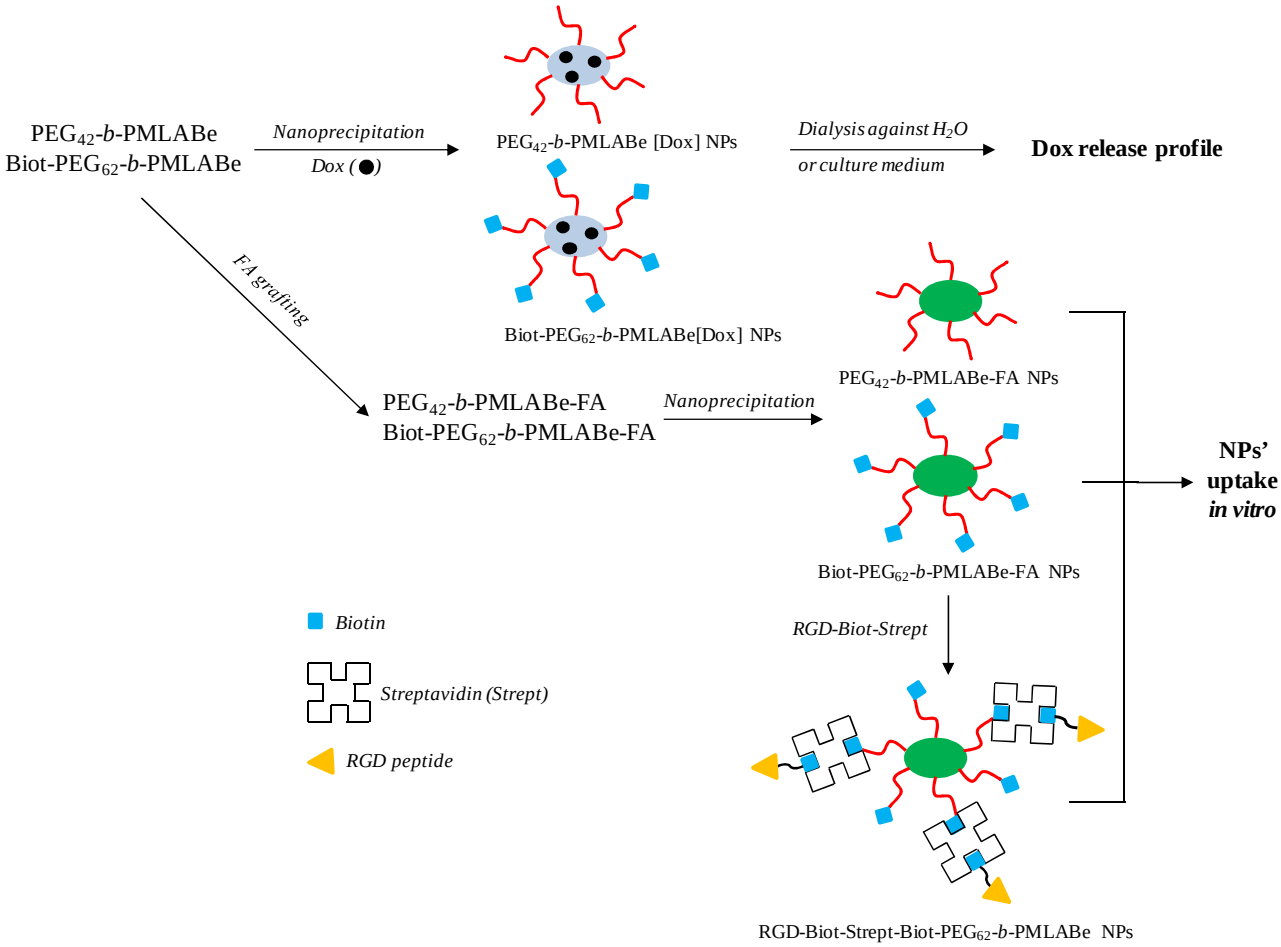

653

654

655 Figure 2.

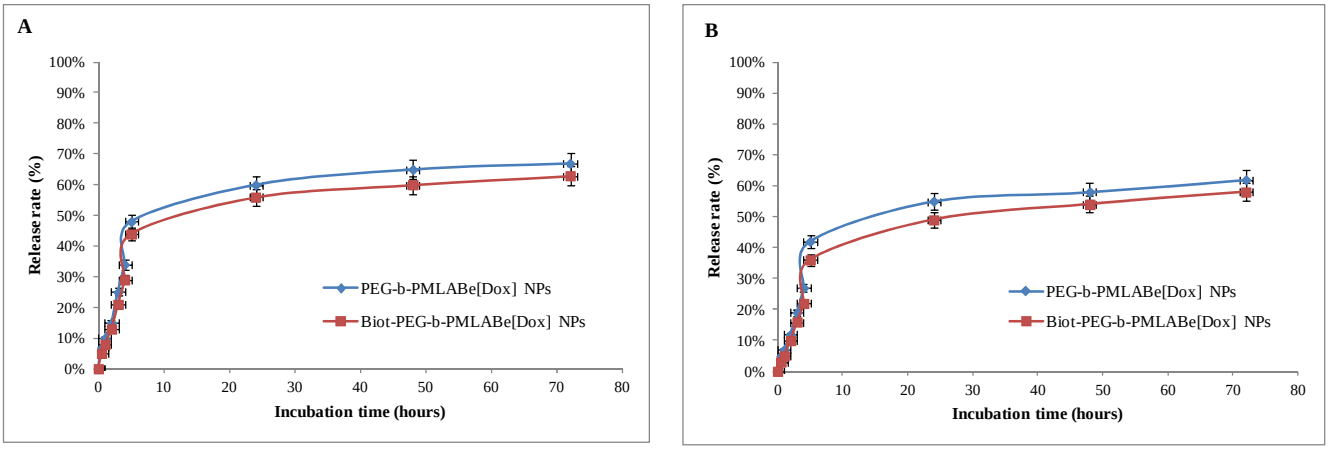

656

657

Figure 3.

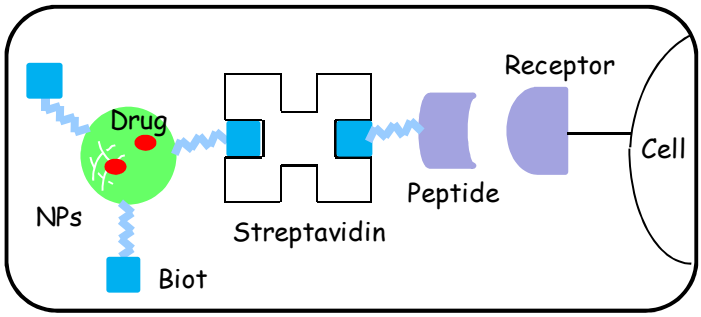

666 Figure 4.

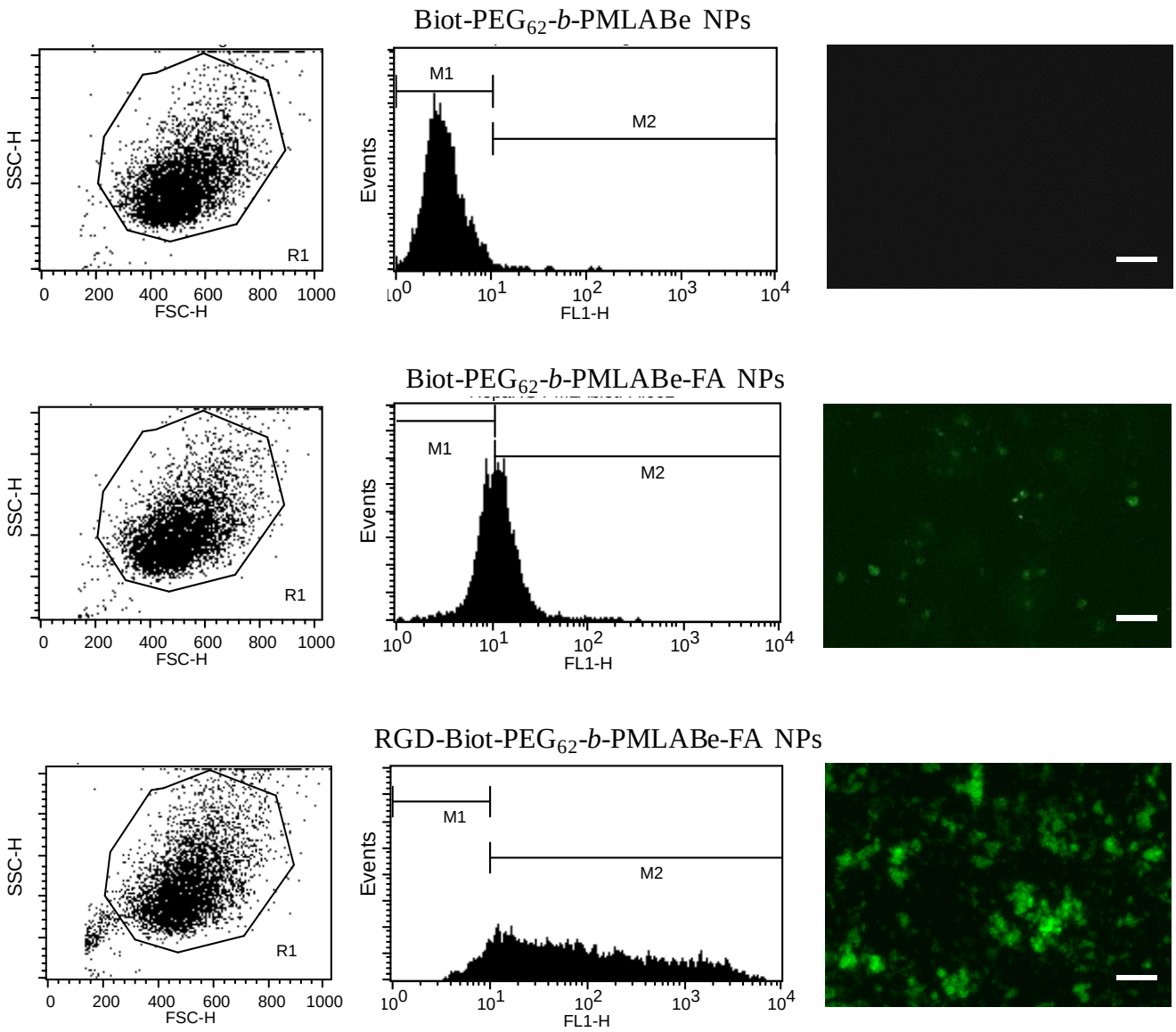

667

668

669 Figure 5.

670

671

672

673

674

675

676

677

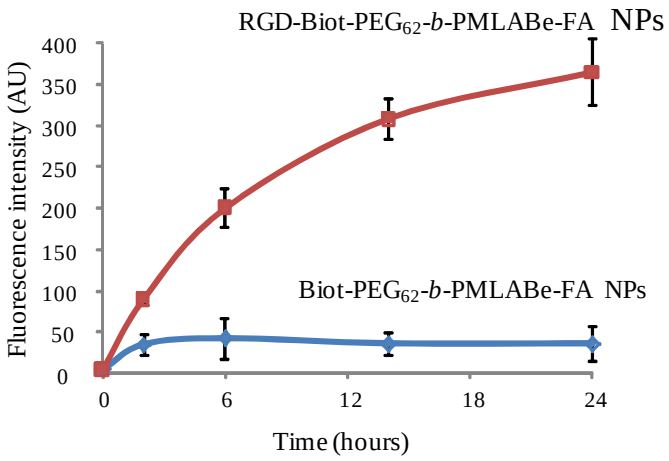

Figure 6.

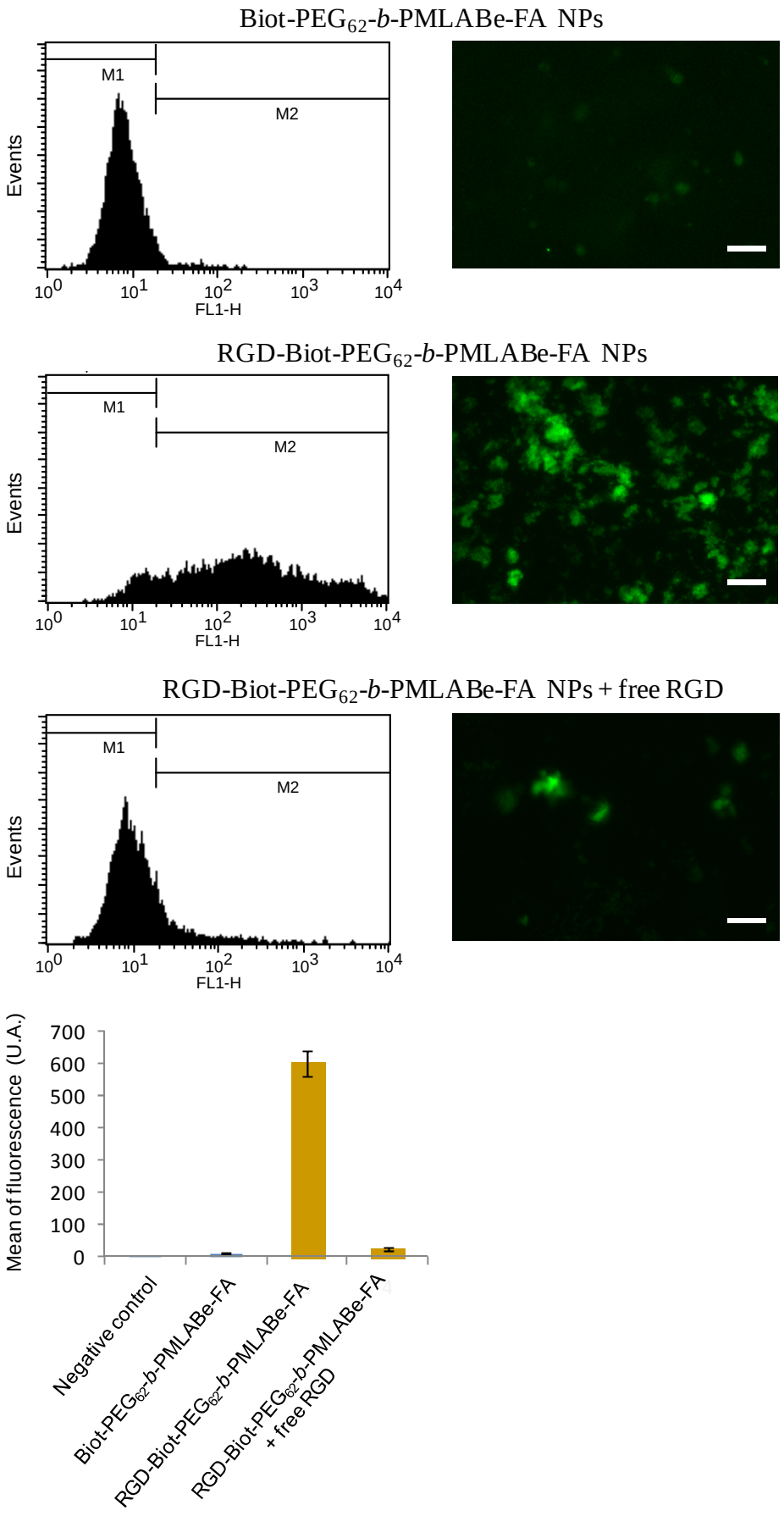
Biot-PEG62-b-PMLABe-FA NPs
M1
M2
Events
FL1-H
RGD-Biot-PEG62-b-PMLABe-FA NPs
RGD-Biot-PEG62-b-PMLABe-FA NPs + free RGD
Mean of fluorescence (U.A.)
Negative control
Biot-PEG62-b-PMLABe-FA
RGD-Biot-PEG62-b-PMLABe-FA
RGD-Biot-PEG62-b-PMLABe-FA + free RGD

704 Figure 7.

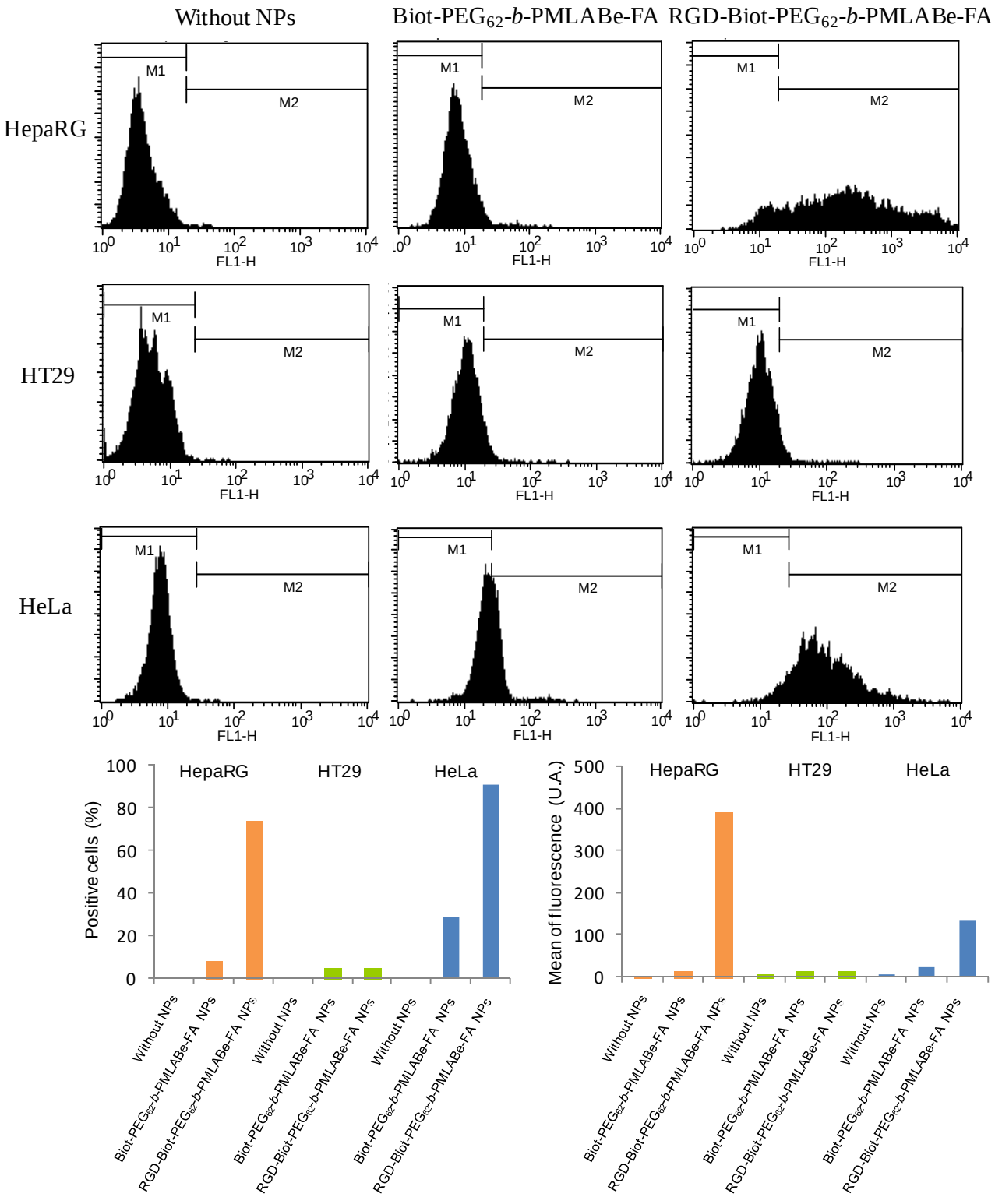

705

706

Scheme captions

Scheme 1. Synthetic route to FA grafted PEG_{42}-b-PMLABe and Biot-PEG_{62}-b-PMLABe.

711 Scheme 1.

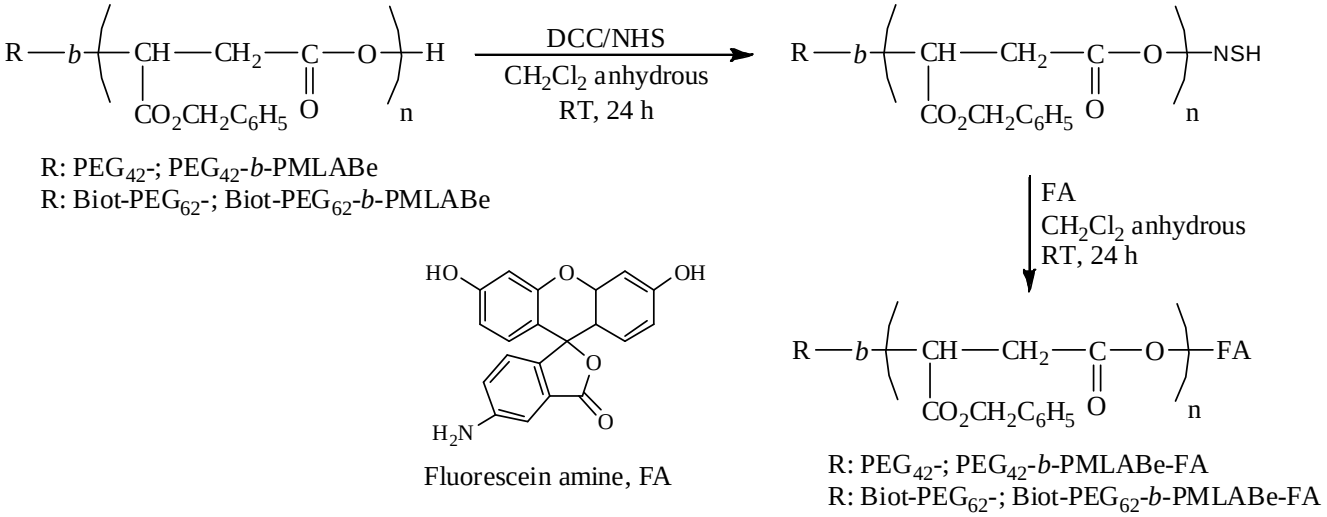

712